Ship-motion Green function with viscous effect

Xiaobo Chen[1,2], **Hui Liang**[3] and **Young-Myung Choi**[1]

[1]Research Department, Bureau Veritas Marine & Offshore, Paris, France
xiaobo.chen@bureauveritas.com

[2]College of Shipbuilding Engineering, Harbin Engineering University, Harbin, China

[3]Technology Centre for Offshore and Marine, Singapore (TCOMS), 118411, Singapore

The fundamental solution (Green function) of free-surface flows associated with fluid *viscosity* is studied by examining the complex dispersion relation and evaluating time-harmonic ship waves generated by a pulsating and translating source at the free surface. Being critically important, the viscous effect indeed removes the peculiar singularity and fast oscillations in the Green function when the field point approaches to the track of the source located close to or at the free surface.

1 Introduction

The Green function associated with a pulsating and translating source represents the fundamental solution to ship-motion problems with forward speed. Many studies have been carried out to analyse its behaviours and to develop numerical schemes for its computations. The most striking property is the peculiar singularity and fast oscillations for field points approaching to the track of source point at or close to the free surface, as revealed in Chen & Wu (2001). This behaviour makes the waterline integral included in classical boundary integral equations nightmarish. Manifestly non-physical, it becomes the stumbling block to prevent from developing a reliable tool to evaluate wave loads and induced ship motions.

Not satisfied with using practical treatments by lowering the waterline or by parametrising numerical filters to mask the difficulty, we have examined the origin of besetting by re-introducing the neglected physical parameters like surface tension, fluid viscosity or combination of both. The present paper concerns the introduction of viscosity. Unlike the classical way introducing "fictitious" viscosity (Rayleigh viscosity or Lighthill's argument) which was just a mathematical device to make waves propagating radially outwards, the analysis based on linearised Navier-Stokes equation and Helmholtz decomposition in Chen & Dias (2010) leads to the consistent kinematic and dynamic boundary conditions on the free surface with viscosity. The particular case of oscillating Stokelet (equivalent to pulsating singularity) is considered in Lu (2019) and that of translating source in Liang & Chen (2019).

The dispersion relation associated with the boundary condition on the free surface with viscosity is complex with an imaginary part proportional to the viscosity and a three-fold derivative (once with respect to the time and twice to the vertical coordinate) of velocity potential. The analysis of the complex dispersion equation gives complex wavenumbers with increasing imaginary part and shows that waves of small wavelength are heavily damped and the peculiar singularity disappears. Time-harmonic waves generated by a translating and pulsating source at the free surface are illustrated in the paper.

2 Complex dispersion relation with viscosity

We use the reference system moving with the ship of length L whose ox-axis points to the direction of ship speed U, xoy-plane on the mean free surface and oz-axis positive upwards, and define following parameters

$$F = U/\sqrt{gL}\,, \qquad f = \omega\sqrt{L/g}\,, \qquad \tau = Ff = U\omega/g \tag{1}$$

where g is the acceleration due to gravity and ω the encounter frequency.

The fundamental solution to the time-harmonic ship-motion problem is classically defined as the real part $\Re\mathrm{e}\{G(\boldsymbol{x},\boldsymbol{\xi})\mathrm{e}^{-\mathrm{i}ft}\}$ in which the spatial Green function $G(\boldsymbol{x},\boldsymbol{\xi})$ is decomposed into :

$$4\pi G(\boldsymbol{x},\boldsymbol{\xi}) = -1/r + 1/r' + G^F(\boldsymbol{x},\boldsymbol{\xi}) \tag{2}$$

in which r is the distance between the source point $\boldsymbol{\xi}(\xi, \eta, \zeta)$ and the field point $\boldsymbol{x}(x, y, z)$ and r' is that between the mirror source $\boldsymbol{\xi}'(\xi, \eta, -\zeta)$ and $\boldsymbol{x}(x, y, z)$. The free-surface term $G^F(\boldsymbol{x}, \boldsymbol{\xi})$ is given by the Fourier representation

$$F^2 G^F(\boldsymbol{x}, \boldsymbol{\xi}) = \frac{1}{\pi}\int_{-\pi}^{\pi} \mathrm{d}\theta \int_0^{\infty} \mathrm{d}k \, \frac{k}{\mathcal{D}(k, \theta)} \mathrm{e}^{k(v - \mathrm{i}w)} \tag{3}$$

with the speed-scaled Fourier variable k and

$$v = (z + \zeta)/F^2 \leq 0 \quad \text{and} \quad w = \cos\theta(x - \xi)/F^2 + \sin\theta(y - \eta)/F^2 \tag{4}$$

The denominator of the integrand function in (3) is the dispersion function associated the boundary condition (eq.16) in Chen & Dias (2010) :

$$\mathcal{D}(k, \theta) = D(k, \theta) - \mathrm{i}4\epsilon(k\cos\theta - \tau)k^2 \quad \text{with} \quad D(k, \theta) = (k\cos\theta - \tau)^2 - k \tag{5}$$

The coefficient ϵ in (5) is defined by

$$\epsilon = \nu/(F^3\sqrt{gL^3}) = \nu g/U^3 \tag{6}$$

where ν denotes the fluid kinematic viscosity.

The real part of $\mathcal{D}(k, \theta)$ given in (5) is exactly the same as the classical dispersion function $D(k, \theta)$. Both the complex dispersion function $\mathcal{D}(k, \theta)$ and its real pair $D(k, \theta)$ are independent of the sign of θ so that we consider only the case $\theta \in (0, \pi)$. The quadratic equation $D(k, \theta) = 0$ has two roots, namely,

$$k^- = \tau^2/(1/2 + \sqrt{1/4 + \tau\cos\theta})^2 \quad \text{and} \quad k^+ = (1/2 + \sqrt{1/4 + \tau\cos\theta})^2/\cos^2\theta \tag{7}$$

Unlike the way to add an artificial and infinitesimal imaginary part (equivalent to $\epsilon \to 0^+$) multiplying a sign function $\mathrm{sgn}(D_f)$, the complex dispersion function (5) represents the exact viscous effect. The cubic dispersion equation $\mathcal{D}(k, \theta) = 0$ gives three complex roots denoted by :

$$k_{1,2,3}(\theta) = \kappa_{1,2,3}(\theta) + \mathrm{i}m_{1,2,3}(\theta) \tag{8}$$

The first wavenumber k_1 is of finite value. Its real part κ_1 is very close to k^- and its imaginary part $m_1 > 0$. The second wavenumber k_2 is very different in its imaginary part $|m_2| \propto \epsilon 4|\kappa_2|^{5/2}$ while κ_2 can be very large for $\theta \approx \pi/2$, otherwise κ_2 is close to k^+ for $\epsilon \ll 1$. The third wavenumber k_3 has a negative real part $\kappa_3 < 0$ and very large modulus of order $O(1/\epsilon)$. By assuming $\epsilon \ll 1$, we have approximations of

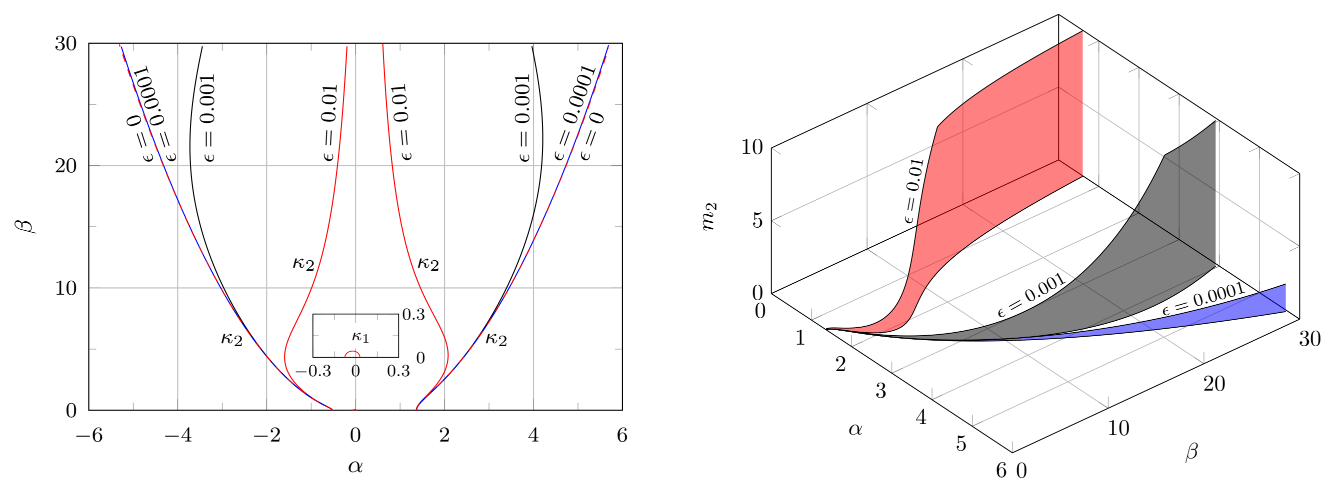

Figure 1: Complex dispersion curves $k_{1,2}(\theta)$ at $\tau = 0.2$: (left figure) real part $\kappa_{1,2}(\theta)$ on the Fourier plane $(\alpha, \beta) = \kappa(\cos\theta, \sin\theta)$ and (right figure) its imaginary part $m_2(\theta)$ by the height above the (α, β) plane.

first two wavenumbers

$$\kappa_1 \approx k^- \qquad m_1 = \epsilon 4(k^-)^{5/2}/(2\sqrt{k^-}\cos\theta + 1) \quad \text{for} \quad \theta \in [0, \pi - \theta_c] \tag{9a}$$

$$\kappa_2 \approx k^+ \qquad m_2 = \epsilon 4(k^+)^{5/2}/(2\sqrt{k^+}\cos\theta - 1) \quad \text{for} \quad \theta \in [0, \pi/2) \tag{9b}$$

$$\kappa_2 \approx k^+ \qquad m_2 = \epsilon 4(k^+)^{5/2}/(2\sqrt{k^+}\cos\theta + 1) \quad \text{for} \quad \theta \in (\pi/2, \pi - \theta_c] \tag{9c}$$

in which the particular value $\theta_c = 0$ for $\tau \leq 1/4$ and $\theta_c = \arctan(\sqrt{16\tau^2 - 1})$ for $\tau > 1/4$. For $\theta \in (\pi - \theta_c, \pi]$, we use the complex wavenumbers derived from $D(k, \theta) = 0$, i.e.

$$\kappa_1 = \kappa_2 = (1/2 + \tau \cos\theta)/\cos^2\theta \qquad m_1 = -m_2 = \sqrt{-1/4 - \tau\cos\theta}/\cos^2\theta \tag{9d}$$

since the terms of order $O(\epsilon)$ can be neglected in this interval. Furthermore, we ignore the contribution of large third wavenumber $k_3 = O(1/\epsilon)$ which has a negative real part.

The complex wavenumbers $k_{1,2}(\theta) = \kappa_{1,2}(\theta) + \mathrm{i}m_{1,2}(\theta)$ are illustrated by the curves in the Fourier plane $(\alpha, \beta) = \kappa(\cos\theta, \sin\theta)$ on the left of Figure 1 for the real part $\kappa_{1,2}(\theta)$ and by the height above the (α, β) plane for the imaginary part $m_2(\theta)$ on the right of Figure 1. The value of $\kappa_1(\theta)$ is small and around the origin, depicted by the zoomed box in the middle of left picture. Several values of $\epsilon = 10^{-2}, 10^{-3}, 10^{-4}$ and $\epsilon = 0^+$ (without viscosity) are used. The dispersion curve at $\epsilon = 10^{-4}$ is not distinguishable with that without viscosity in real plane but the imaginary m_2 is not negligible. Higher the value of ϵ is, more rapidly the imaginary part increases.

3 Ship-motion Green function

The integrand function $k/\mathcal{D}(k, \theta)$ in (3) is a meromorphic function and can be decomposed into the sum of three fractions associated with the three roots. The inner k-integral of G^F can then be integrated in a closed form and (3) is re-written as :

$$F^2 G^F(\boldsymbol{x}, \boldsymbol{\xi}) = \frac{1}{\pi}\int_{-\pi+\theta_c}^{\pi-\theta_c} \frac{\kappa_2\mathcal{K}_2(\theta) - \kappa_1\mathcal{K}_1(\theta)}{2\sqrt{1/4 + \tau\cos\theta}}\,\mathrm{d}\theta + \frac{\mathrm{i}}{\pi}\int_{\pi-\theta_c}^{\pi+\theta_c} \frac{k_2\mathcal{K}_2(\theta) - k_1\mathcal{K}_1(\theta)}{2\sqrt{-1/4 - \tau\cos\theta}}\,\mathrm{d}\theta \tag{10}$$

with an error of order $O(\epsilon)$, as the third term relative to k_3 is neglected. The wavenumber-integral function $\mathcal{K}(\theta)$ involved in (10) is defined by

$$\mathcal{K}(\theta) = \int_0^\infty \frac{\mathrm{e}^{k(v - \mathrm{i}w)}}{k - (\kappa + \mathrm{i}m)}\,\mathrm{d}k = \mathbf{Cex}(\mathcal{Z}) + \mathrm{i}\pi\left[\mathrm{sgn}(m) + \mathrm{sgn}(mv - \kappa w)\right] H(\kappa)\exp(\mathcal{Z}) \tag{11}$$

with

$$\mathbf{Cex}(\mathcal{Z}) = \mathrm{e}^{\mathcal{Z}} E_1(\mathcal{Z}), \quad \mathcal{Z} = (\kappa + \mathrm{i}m)(v - \mathrm{i}w) \tag{12}$$

and (v, w) defined by (4) while (κ, m) representing (κ_1, m_1) or (κ_2, m_2). Furthermore, $\mathrm{sgn}(\cdot)$ is the sign function and $H(\cdot)$ the Heaviside function. Finally, $E_1(\cdot)$ is the exponential-integral function defined by (eq.5.1.1) in Abramowitz & Stegun (1967). The modified exponential-integral function $\mathbf{Cex}(\cdot)$ is a non-oscillatory function and its θ-integration yields then a non-oscillatory local component.

Since $\mathcal{Z}$ defined by (12) is complex, the function $\exp(\mathcal{Z})$ on the right hand side of (11) is oscillatory. The θ-integration of $\exp(\mathcal{Z})$ gives the wave component if any and could contribute to the non-oscillatory local component as well. In the analysis of Chen & Noblesse (1997), an original relationship between the dispersion curves in real Fourier plan and the far-field wave patterns was established. According to this analysis and the picture of dispersion curves on the left of Figure 1, the wave patterns are not affected for small $\epsilon \ll 1$ and could be largely modified for larger ϵ, i.e., for slow forward speed or in high viscous fluid, according to the definition (6). What is important is, according to (9), that the value of imaginary wavenumber $|m_2| \approx \epsilon 4(k^+)^{5/2}$ becomes very large for $\theta \approx \pi/2$. The second part of the wavenumber-integral function (11) is derived such that the real part of $\mathcal{Z}$ is always negative $\Re\mathrm{e}\{\mathcal{Z}\} = \kappa v + mw < 0$ when the sign of m_2 and that of imaginary part $\Im\mathrm{m}\{\mathcal{Z}\} = mv - \kappa w$ are the same. Even for $v = 0$, the magnitude of $|\exp(\mathcal{Z})| = \mathrm{e}^{\kappa v + mw}$ decays exponentially, and waves of large wavenumbers k^+ are heavily damped or disappear simply. The peculiar singularity and fast oscillations predicted in Chen & Wu (2001) are then removed by introduction of fluid viscosity.

4 Discussion and conclusions

Although the appearance of sign and Heaviside functions in (11), the wavenumber-integral function $\mathcal{K}(\theta)$ is a smooth function of θ for $v < 0$ but has sharp variation at $\theta \approx \theta_0$ and $\theta = \theta_0 + \pi$ with θ_0 defined by

$$\theta_0 = \arctan[-(x - \xi)/(y - \eta)] \tag{13}$$

At $v = 0$, the wavenumber-integral function $\mathcal{K}(\theta)$ and its derivatives are singular at $\theta = \theta_0$ and $\theta = \theta_0 + \pi$ so that special algorithms are needed to extract the singular terms and to integrate them analytically. Furthermore, the highly oscillatory variation of $\mathcal{K}(\theta)$ for large θ (approaching to $\pi/2$ for small ϵ) should

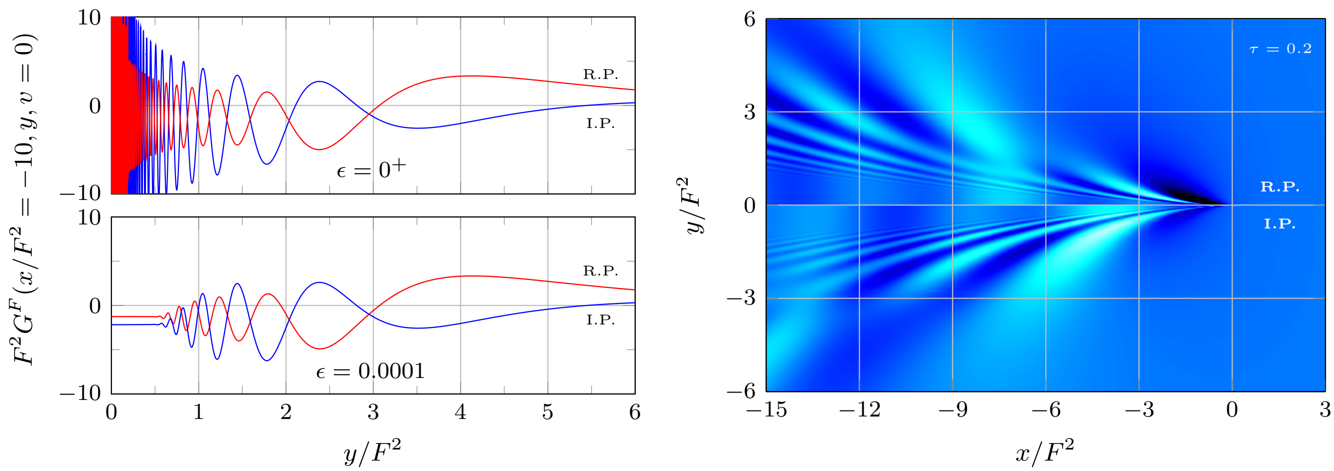

Figure 2: Time-harmonic $G(\boldsymbol{x}, \boldsymbol{\xi})$ at $\tau = 0.2$ along a strait cut at $(x - \xi)/F^2 = -10$ and $v = 0 = z + \zeta$ without viscosity (left top) and with viscosity (left bottom) and patterns (right) generated by a source at the free surface.

be integrated with cautions.

The free-surface term $G^F(\boldsymbol{x}, \boldsymbol{\xi})$ defined by (10) is illustrated on Figure 2. Its real (R.P.) and imaginary parts (I.P.) along a strait cut at $(x - \xi)/F^2 = -10$ on the free surface $v = (z + \zeta)/F^2 = 0$ are depicted by red and blue solid lines, respectively, on the left. The pulsating and translating source is located at the origin for $\tau = 0.2$. The top part represents the values without viscosity ($\epsilon = 0^+$) while the bottom part depicts the values with viscosity ($\epsilon = 0.0001$). The singular and fast oscillations in the vicinity of source track (top) disappear with viscosity (bottom). On the right of Figure 2, the wave pattern is depicted with the real part and imaginary part on the up half and lower half, respectively.

The viscous effect analysed through the complex dispersion relation is shown to be primordial for the fundamental solution to be physically acceptable and numerically calculable. The new ship-motion Green function with viscosity should be critically useful in the computation of integrals along the waterline or/and on the free surface to solve the ship seakeeping problems with full satisfaction.

Acknowledgements

The work has been partially supported by the National Nature Science Foundation of China with ref no.51779054.

References

[1] Chen XB & Wu GX (2001) On singular and highly oscillatory properties of the Green function for ship motions. *J. Fluid Mech.*, 445, 77-91.

[2] Chen XB & Dias F (2010) Visco-potential flow and time-harmonic ship waves. *Proc. 25th IWWWWFB.* Harbin, China.

[3] Lu DQ (2019) Analytical solutions for the interfacial viscous capillary-gravity waves due to an oscillating Stokelet. *J. Hydrodyn.* 31 (6): 1139-1147.

[4] Liang H & Chen XB (2019) Viscous effects on the fundamental solution to ship waves. *J. Fluid Mech.*, 879, 744-774.

[5] Abramowitz M. & Stegun I.A. (1967) Handbook of mathematical functions. *Dover publications.*

[6] Chen XB & Noblesse F (1997) Dispersion relation and far-field waves. *Proc. 12th IWWWWFB.* Marseilles, France.